FrED Factory Control and Design of Experiments

Process Control of the fibre Diameter in a Desktop Extrusion Device (FrED)

Alexander Sparry Brush
Dept. of Mechanical Engineering
Massachusetts Institute of Technology
Cambridge, MA, United States
brusha@mit.edu

Enrique Flores Medina
Dept. of Mechanical Engineering
Massachusetts Institute of Technology
Cambridge, MA, United States
enriquef@mit.edu

***Abstract* — This paper presents improvements and characterization of a Fibre Extrusion Device (FrED). The initial construction involved identifying errors and areas of ambiguity in the assembly instructions, ensuring consistency in manufacturing. To get the device in a state of statistical control, a temperature control system was developed using a Proportional-Integral (PI) controller and Pulse Width Modulation (PWM) to keep the extruder temperature constant. A Design of Experiments (DoE) approach was taken to characterize the effects of extrusion temperature, extrusion speed, and material color on the resulting fibre diameter. Additionally, live Statistical Process Control (SPC) was added to the user interface through the implementation of the Nelson Rules to alert the operator of statistically improbable events, allowing for real-time monitoring and adjustment of the device. This work emphasizes the importance in iterative problem solving and real-time analytics in achieving consistency in fibre extrusion. This work will serve as a baseline and for future research and improvement involving the FrED device.**

Keywords—fibre extrusion; temperature control; design of experiments; statistical process control

I. Introduction

The Fibre Extrusion Device (FrED) Factory at the Massachusetts Institute of Technology (MIT) is a desktop system that mimics the industrial fibre extrusion draw process. It was designed for educational and research purposes, providing a functional device for "hands-on learning in data acquisition, control systems, and smart manufacturing" [6].

Traditional fibre optic draw processes are multiple stories high and very complex. The FrED device condenses this process into one small device which can be used for many educational experiments. The FrED device costs less than $200, and aims to make learning about manufacturing more accessible to students.

FrED devices are built on campus at MIT in a laboratory called the FrED Factory; designed for students to learn about manufacturing and to get hands-on experience assembling the device. The lab serves as a facility for students to learn optimization and design-for-manufacturing, while also being a space for research.

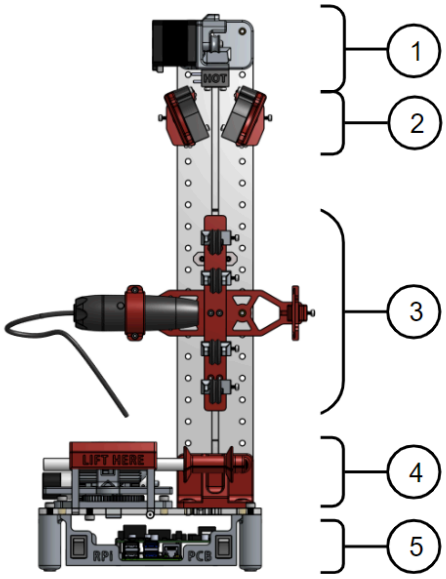

Figure 1. Diagram of a FrED device.

Figure 1 shows a diagram of the FrED device, highlighting the main subsystems within the design. The first subsystem is the extruder. This subsystem consists of a stepper motor which feeds material into a heating block which has a thermistor to measure the temperature. Once melted, the material is fed into the nozzle where it is stretched into a fibre.

The second subsystem is for fibre cooling. As the hot fibre is extruded, it is fed past two radial blower fans which cool the material before it is processed in the following subsystems.

The diameter measurement subassembly follows, using a camera to measure the diameter of the fibre. In this subsystem, the fibre is fed through a series of ball bearings pulleys to hold it in view of the camera with a black sheet of cardstock behind it for an accurate measurement reading.

The fibre is then fed into the fourth subsystem where it is collected on a spool which is driven by a DC motor. The DC motor is connected to a gearbox which gives the spool rotational motion and oscillating linear motion. This motion allows for the fibre to be uniformly spooled.

Finally, the electronics are held at the bottom of the FrED. The FrED device is run using a custom Printed Circuit Board (PCB) and a Raspberry Pi 4. These electronics control the device and a user interface was developed where many parameters can be changed while the device is running. The user interface also provides live updates on important parameters such as temperature, motor speed, and diameter. The diameter output is the most important and is used as the main reference point when determining if the device is functioning properly.

II. Methodology

A. FrED Assembly

The first step of the project was to assemble two FrED devices to be used for the project. One goal of the FrED Factory lab at MIT is to create a structured assembly process to allow for rapid production of FrEDs. Assembling FrEDs gave insight into where this process worked well and where it needed to be improved. Each FrED was assembled by a different researcher, meaning that the final devices could be compared to find variation which resulted from unclear instructions. The majority of the hardware consisted of 3D printed parts, which are cheap to manufacture and easy to redesign and update.

The hardware assembly began with the gearbox subassembly, located at the base of the device where the fibre is spooled. The gearbox was assembled using a jig which held many parts together while the gears were attached and aligned. This assembly step was time consuming, but relatively seamless. However, tolerance issues between 3D printed parts were noticed between the first and second assembly.

The second step of the hardware assembly was the cooling subassembly, which consisted of attaching two fans to a bracket. These fans blow air at the hot fibre, cooling it before it runs through the rest of the device. The steps in this process were clear and this step was very quick to complete.

The extruder subassembly was then created, which housed a stepper motor that fed the stock material into a heating unit which melted the material and pushed it through a small nozzle to create the fibre. In this step, there were a few unclear instructions, but the process was not difficult or time consuming.

The last subassembly made was the camera assembly, which held the camera next to ball bearings which aligned the fibre in view. A black background was also held behind the fibre so the camera can get an accurate diameter measurement. This step did not have any instructions for where to place the ball bearings, and the effect of this on the output diameter is unknown.

Finally, all of the subsystems were attached to the frame, which was constructed from plexiglass parts mounted together with 3D printed brackets. When attaching parts to the frame, the instructions were often unclear, resulting in the two FrEDs having parts mounted at different locations. Overall, the main areas of confusion within the hardware assembly resulted from unclear instructions, unspecified mounting locations, and tolerance issues.

After the hardware was assembled, the electronics needed to be connected. FrED is controlled by a Raspberry Pi 4 and a custom PCB. Many parts, such as the switches and connectors, needed to be soldered to the circuit board, but there were no instructions for how to do this. Instead, a completed FrED was used as a template and the wiring was copied. This step was very time consuming, taking over six hours to wire both FrEDs.

Once both FrEDs were fully assembled, they were turned on and it was found that one of the devices did not work. The issue was investigated and it was determined that a faulty thermistor was resulting in the error. Due to time constraints, the project was continued with one FrED.

B. Initial Assessment of FrED

An experiment was performed to provide an initial assessment regarding the normality of the fibre diameter measurements. For this purpose, the existing PID controller for temperature was utilized with its default target of 95º C, and with an extrusion motor speed of 1.2 RPM.

A normal probability plot of the diameter measurements obtained in this experiment can be observed in Figure 2, where the distribution is clearly not Gaussian.

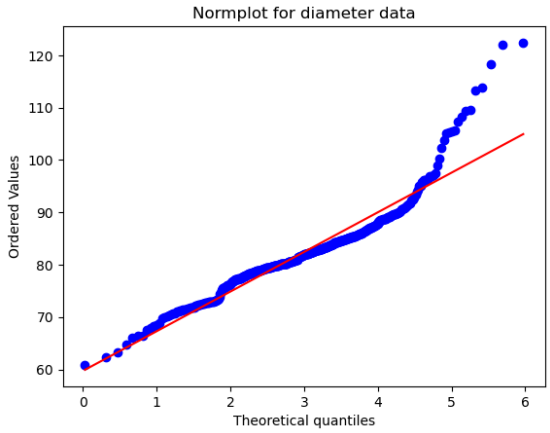

Figure 2. Normal probability plot for initial assessment.

The first thing to note is the range of values obtained for the diameters, which goes around 60 to 130. This, as discussed with the FrED factory team, is the result of not calibrating the camera. To do it, a cylinder with a known diameter is needed, however, the laboratory did not have it when the experiments took place. Hence, it was decided to utilize the uncalibrated measurements, given that the same scaling factor will propagate throughout every experiment.

As for the non-normal behavior, it was observed in the experiments that the fibre preform would not melt evenly, generating large blobs periodically. Figure 3 shows this behavior, which could have caused the normal probability plot in Figure 2 to have two different linear regions: one for the

real fibre diameter distribution and a second one for the blob diameter distribution.

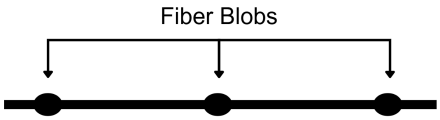

Figure 3. Blobs formed in the fibre.

Furthermore, it was observed that the device would vibrate with the spool movement, making both the extruded fibre and the camera become unstable. As a result, this added more noise to the diameter measurements.

Upon talks with the FrED factory team, it was determined that vibrations could be reduced by adding grease to the gearbox and smoothing edges and borders that generated significant friction, but their entire removal was an unattainable task. As the device is meant to be transportable and all its components are attached to the base, the FrED frame essentially acts as a large cantilever beam that is highly sensitive to movement.

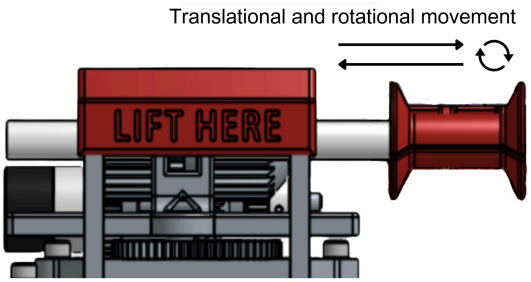

Figure 4. Main source of vibrations in FrED.

Therefore, the best alternative was to scrub the diameter data, eliminating the affected measurements. This method involved the removal of zeroes and Not a Number (NaN) values, as well as manually selecting regions that had infeasible diameter values and were clearly the result of vibrations. These were close-to-zero values and their neighbors, as vibrations would affect multiple measurements. An example of applying the method is seen in Figure 5, where the highlighted areas were removed.

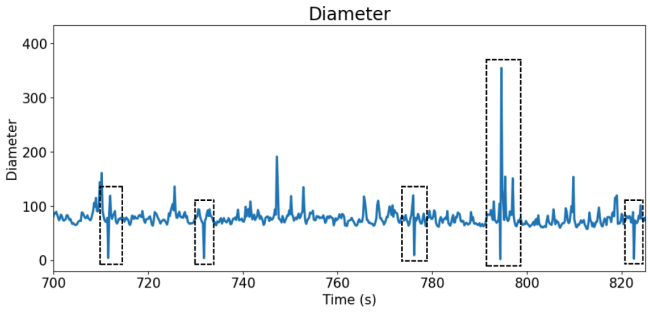

Figure 5. Example of data scrubbing due to FrED vibrations.

This method, although imperfect, allowed for a proper evaluation of the process. Hence, it was used to generate the normal probability plot shown in Figure 2. It is important to note that large values were not removed initially, as they could be attributed to the formation of blobs. However, when blobs were eliminated from the process, very large diameters were also scrubbed from the data.

From this initial analysis, a characterization of FrED was required to identify the sources causing the non-normal behavior of the system, mainly through the generation of blobs. The steps followed for this are presented in the next section.

C. *FrED Characterization*

To achieve a desired diameter output, an understanding of the different subsystem behaviors that make up FrED was fundamental. For this purpose, three factors that play a crucial role in these subsystems were identified and explored.

1. Fibre Materials
2. Extrusion Motor Speed
3. Extrusion Temperature

Factors such as the fan speed in the cooling subsystem, and camera frame rate in the measurement subsystem were not considered in the analysis, as the FrED factory team mentioned they could not be changed or had no significant impact.

The fibre materials were fixed to hot melt glues - mainly composed of polymers, resins, and wax - of two distinct types: white and clear. It was hypothesized that they could produce different diameters for equal machine parameters, but that no deterministic changes could occur due to using different materials. Hence, there were no further explorations on material usage.

The extrusion motor was a NEMA 17 Stepper Motor, characterized by having 200 steps per revolution and a step accuracy of $\pm$ 5% [5]. Per the extrusion process, the motor speed was fixed at particularly low levels, rotating at a maximum rate of 1.5 RPM which yields better step accuracy [4]. Given this, coupled with a maximum error of 0.09º per step, which cannot accumulate as the steps are fixed, the extrusion motor speed was excluded as a potential source of non-controlled deterministic change in the output diameter.

Finally, the temperature was examined. There are three components to this: a thermal switch, a thermistor, and a heating block. The thermal switch ensures that the temperature does not exceed 105º C by shutting down the heating block. The thermistor is used to monitor the heating block's temperature through changes in resistance. The heating block is used to melt the preform and create the fibre.

An on/off PID controller was initially employed by the FrED factory team to achieve a desired input temperature, with results shown below. This controller also utilized a moving average on the thermistor temperature readings with a window size of 8, reducing the noise from the measurements. However, with the constant oscillations exhibited in the temperature levels, blobs regularly formed in the fibre.

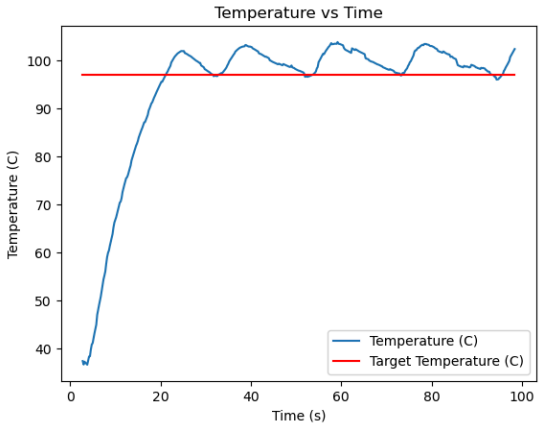

Figure 6. On/off PID temperature controller.

To mitigate this effect, a first decision to introduce a voltage regulator was made. This reduced the maximum current that could be supplied to the heating block, reducing the constant overshooting effect seen in Figure 6. As the voltage was stepped down from 12V to 7V, the current was limited by a factor given in equation (3):

$$I_0 = 12v/R \quad (1)$$

$$I_1 = 7v/R \quad (2)$$

$$I_1/I_0 = 7/12 \approx 0.58 \quad (3)$$

With this new addition, the temperature had a significantly smaller overshoot, as seen in Figure 7.

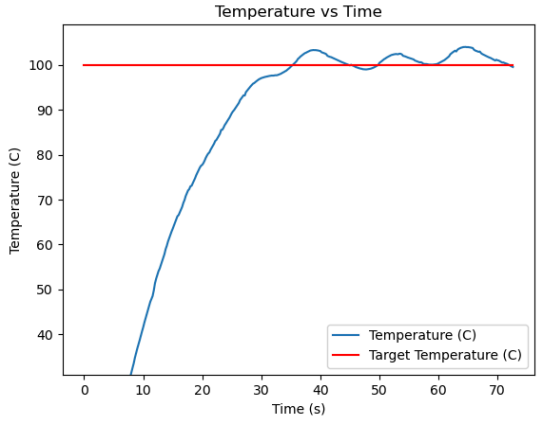

Figure 7. On/off PID temperature controller with voltage regulation.

Note: The y-axes were adjusted to standardize across all the plots, nevertheless, not all temperatures started at the same point due to the nature in which the experiments were performed.

The overshooting, however, was still present. In an attempt to mitigate this issue, a controller with a fixed number of off-signals for every on-signal was implemented. The purpose was to manually enforce rules on how often the heater could be activated, as the thermistor would not provide feedback to the controller until the temperature had transferred through the heating block. This distance between the components is shown below, where the thermistors' readings are delayed by the conductivity and thickness of the heating block, as well as the distance to the heating source.

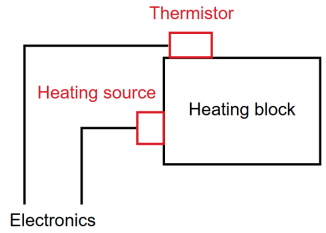

Figure 8. FrED heating block diagram.

As expected, this controller was imperfect. If the temperature was below the target, the number of off-signals sent per cycle could be sufficiently large so as to cause a constant decay in temperature. Furthermore, different operating conditions, such as introducing new, cold raw material, would make this controller fail regularly.

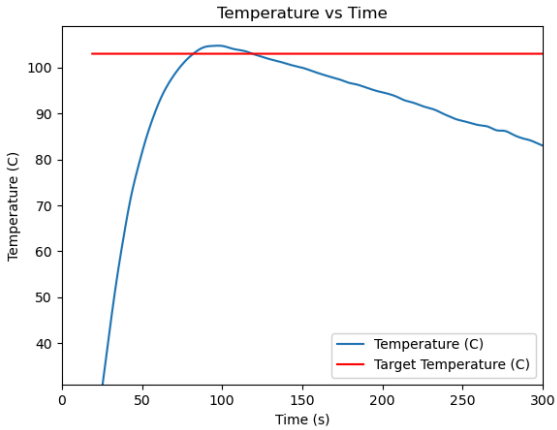

Figure 9. Fixed-cycle on/off temperature controller.

With the findings from this controller, it was determined that a controller on the duty cycle of a Pulse Width Modulated (PWM) signal would prevent the constant overshooting by allowing the controller to provide different voltage levels to the heating block, while also eliminating the constant decay problem from the previous controller.

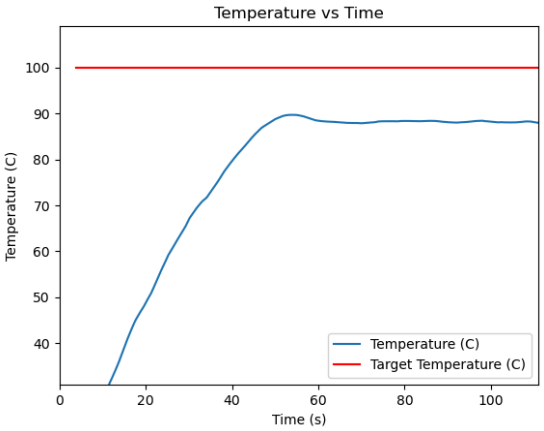

Figure 10. Proportional PWM temperature controller.

The PWM controller achieved stability, but with an approximate error of 20º C. The addition of an integrator term to the controller, effectively converting into a PI controller, fixed the issue and resulted in the finalized temperature controller shown in Figure 11.

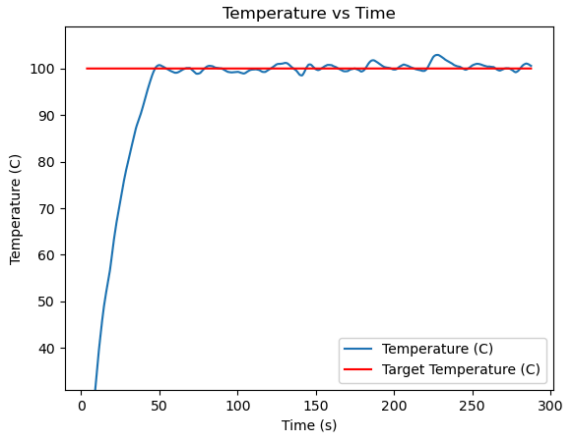

Figure 11. PWM PI temperature controller.

As no more sources of potential variation in the diameter output were identified, a number of brief experiments were run, validating that the measurements followed a normal distribution. More comments can be found in the results section, however, this ensured that the conditions for designed experiments were met.

D. Full Factorial Design of Experiments

Once the FrED device was characterized, it was important to develop a model to predict how various inputs change the diameter. On the FrED device, there are three variable input parameters: material, temperature, and extrusion speed. There are two variations of the hot glue material, white and clear, and it was unknown if using one or the other impacted the results. The white pigment within the glue stick may have unintended effects on the material, potentially affecting viscosity, temperature, or other properties, and therefore it is expected that this may impact the diameter output. The viscosity of the glue decreases as temperature increases, and for this reason the temperature was an important variable to change. Finally, the extrusion speed was varied because this affects the amount of time the material spends in the heater as well as the amount of time that the fibre is cooled in front of the fan. This variable is related to the speed of the spooling motor, which is calculated using the continuity equation below:

$$A_1 v_1 = A_2 v_2 \tag{4}$$

In equation (4), A is defined as the cross section area on one side of the nozzle where v is the velocity of the material on that side of the nozzle. The area of the stock material is calculated using the diameter, and the area of the fibre is calculated using a target diameter of half a millimeter. The motors are programmed by inputting revolutions-per-minute, and therefore the velocity needs to be calculated from this input.

$$v = RPM(\tfrac{2\pi}{60})r \tag{5}$$

Equation (5), calculates velocity, v, using the RPM of the motor and the radius of the shaft that is being rotated. In this equation, the angular velocity, RPM, is converted into units of radians per second, which is then multiplied by the radius to obtain the radial velocity. Substituting (5) for both velocities in (4) and inputting the correct values results in the following equation:

$$RPM_{spooler} = 143.73\, RPM_{extruder} \tag{6}$$

Equation (6) calculates the input speed of the spooler motor based on the input speed of the extruder motor, and it is seen that they are proportionally related.

With three variables, a 2^3 full factorial experiment was decided on because the FrED device outputs a large amount of data quickly and there was a negligible cost per experiment. This designed experiment had 8 tests, but two replicates were run for each test, resulting in a total of 16 recordings. Each of the 8 runs tested every combination of variables, where each variable had a high and low value. The high and low values for each variable are below:

TABLE I. DoE Variables

Variable	***Low [-1]***	***High [1]***
A = Temperature	100º C	105º C
B = Extruder Speed	0.3 RPM	1.2 RPM
C = Material Color	White	Clear

The variables in Table I were determined by running the FrED device and varying the parameters to see what range of values resulted in consistent outputs. The two material colors were observed to behave differently at various temperatures, and therefore the temperature range that worked well for each was smaller than anticipated.

TABLE II. DoE Experiments

Run	***A***	***B***	***C***
(1)	-1	-1	-1
a	1	-1	-1
b	-1	1	-1
ab	1	1	-1
c	-1	-1	1
ac	1	-1	1
bc	-1	1	1
abc	1	1	1

Table II shows all of the designed tests. The rows show each test and the columns show the variables. For example, test *ab* has a high value for variables A and B and a low value for C.

TABLE III. DOE RESULTS

Run	*Replicate I*	*Replicate II*
(1)	86.98	88.73
a	97.12	112.34
b	76.69	76.05
ab	98.32	101.44
c	96.09	102.12
ac	82.13	90.75
bc	90.28	92.82
abc	80.72	81.08

Table III documents the results from each experiment. The FrED device records a diameter every 100 milliseconds, and therefore each experiment had a large number of recordings. To calculate the final value in Table III, 200 points were averaged.

It is important to note that the output diameter is currently unitless, as the FrED Factory did not have the equipment to calibrate the camera when this project happened. This does not affect the analysis because once calibrated, all of the output values can be scaled proportionally to change from unitless to the desired unit.

Applying a linear regression model to the data resulted in the following equation:

$$Y = 86.60 + 0.75A + 1.68B + 0.32AB + 2.13C - 3.99AC - 0.76BC - 1.67ABC \quad (7)$$

Equation (7) may be overfitting the data, and therefore an Analysis of Variance (ANOVA) table was created to test the statistical significance of each regression term. The ANOVA table is shown below:

TABLE IV. REGRESSION ANOVA

Source	*SS*	*d.o.f.*	*MS*	*F0*	*P-value*
Mean	120003	1	120003	41322	0.000
A	8.86	1	8.86	3.06	0.118
B	45.16	1	45.16	15.55	0.004
AB	1.63	1	1.63	0.56	0.476
C	72.59	1	72.59	25.00	0.001
AC	254.24	1	254.24	87.55	0.000
BC	9.33	1	9.33	3.21	0.111
ABC	44.49	1	44.49	15.32	0.004
ε	23.23	8	2.90	–	–
Total	**120462**	**16**	**7528**	–	–

In Table IV, the source column shows the regression term which is being tested. The following columns are sum of squares, degrees of freedom, mean square, f-statistic, and p-value, respectively. For each regression term, the sum of squares was calculated using equation (8). The sum of squares associated with the error was calculated using equation (9).

$$SS = an\beta^2 \quad (8)$$

$$SS\varepsilon = \sum_{i=1}^{n} (y_i - \hat{y}_i)^2 \quad (9)$$

In Equation (8), a is the number of unique treatments, n is the number of replicates, and β is the regression coefficient. In Equation (9) the predicted values are subtracted from the observed values, and the results are squared and summed. Using the sum of squares value, the mean square was calculated:

$$MS = \frac{SS}{d.o.f.} \quad (10)$$

Using the mean square values, each F-statistic was calculated to compare the variances between samples. The corresponding p-value represents the probability that an f-statistic is the same or more extreme than the calculated one.

$$F_0 = \frac{MS}{MS\varepsilon.} \quad (11)$$

Using a critical p-value of 0.05, Table IV shows that the regression coefficients corresponding to the mean, B, C, AC, and ABC are statistically significant. The updated regression model is as follows:

$$Y = 86.60 + 1.68B + 2.13C - 3.99AC - 1.67ABC \quad (12)$$

With this model, a question arose as to whether the model behaved quadratically instead of linearly. This was tested by choosing a point within the specified bounds for each variable and comparing it with the model.

TABLE V. QUADRATIC VARIABLES

Variable	*Quad*
A = Temperature	103º C
B = Extruder Speed	0.8 RPM
C = Material Color	White

TABLE VI. QUADRATIC EXPERIMENT

Run	*A*	*B*	*C*
Quad	0.2	0.11	-1

TABLE VII. QUADRATIC RESULTS

Run	*Replicate I*	*Replicate II*
Quad	86.49	86.63

Both temperature and extruder speed were set at values in between the high and low range. Material color was kept as white, because testing a material that was between white and clear was not feasible due to the lab not owning glue that had a smaller amount of pigment.

Once again, an ANOVA table was created to determine the statistical significance of the quadratic term when compared to the regression model. The updated regression model found in Equation (12) was used for this table.

TABLE VIII. QUADRATIC ANOVA

Source	*SS*	*d.o.f.*	*MS*	*F0*	*P-value*
Mean	120003	1	120003	27146	0.000
B	45.16	1	45.16	10.22	0.010
C	72.59	1	72.59	16.42	0.002
AC	254.24	1	254.24	57.51	0.000
ABC	44.49	1	44.49	10.06	0.010
Quad	1.82	1	1.82	0.41	0.536
ε	44.21	10	4.42	–	–
Total	**120466**	**16**	**7529**	–	–

The quadratic sum of squares was calculated using Equation (13):

$$SS_{Quad} = \frac{n_f n_c}{n_f + n_c}(\bar{y}_{Quad} - \hat{y}_{Quad})^2 \quad (13)$$

In Equation (13), *nf* is the number of factorial design points and *nc* is the number of runs at the quadratic point.

Comparing the p-values from Table VIII to the critical p-value of 0.05, the quadratic term was deemed statistically insignificant.

E. Continuous Statistical Process Control

Statistical Process Control (SPC) was the final implementation, added as an online process with live updates. With diameter measurements that had shown normal behavior and a model to explain them using input parameters, an SPC running plot would allow users to detect deterministic changes and investigate their sources.

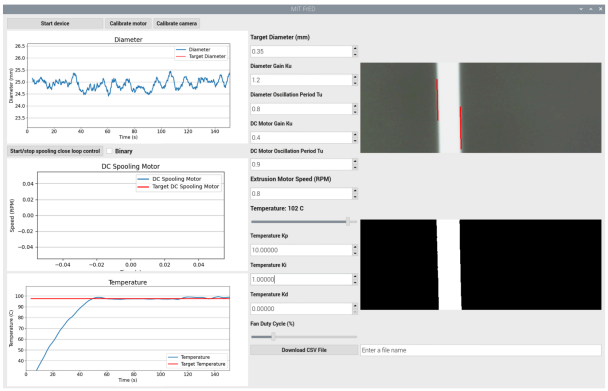

Figure 12. FrED user interface.

A running plot of diameter measurements was already present in the user interface, as shown in Figure 12. The plots worked by sampling the heater temperature and diameter measurements every 100 ms. Then a running average of the last 10 readings was plotted in the live interface, removing sensor noise.

Using these plots, the 8 Nelson Rules were simple to include. As an illustrative example, rule two is presented with corresponding pseudo-code. For better interpretability, a reminder that rule two states:

"Nine (or more) points in a row are on the same side of the mean" [3]

The pseudo-code is shown below. Note that a previous buffer has been defined to store the most recent 14 diameter measurements, such that the analysis is plausible.

```
if buffer length > 8: # Need at least 9 data points
    n_1 = 0; n_2 = 0
    for value in error list: # Defined error as (data point - mean)
        if val > 0: n_1 += 1
        elif val < 0: n_2 += 1
    if n_1 == 9 or n_2 == 9: bad_point = True
```

The interface, with an Upper Control Limit (UCL), a Lower Control Limit (LCL), and a target diameter are presented in Figure 13. It is important to note that, in the absence of historical or phase I data, the grand mean and grand standard deviation were set arbitrarily from visual estimations, hence rule two was broken twice.

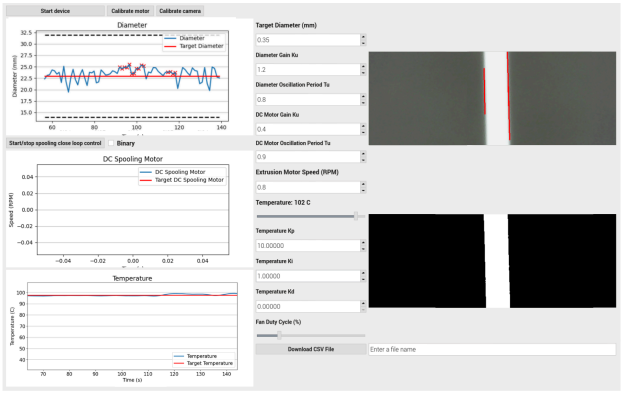

Figure 13. FrED user interface with live SPC.

Nevertheless, for proper usage of real-time SPC, FrED has to run and collect data for a prolonged period of time, establishing a known underlying distribution for the fibre diameter under defined parameters. This process has to be repeated for different combinations of parameters, ensuring that the mean and standard deviation are accurately approximated in every scenario.

III. Results and Future Work

The outlined methodology presented significant improvements to FrED. These are discussed in the order they were obtained, as well as future work recommendations for further improvements.

F. FrED Assembly

The assembly of two FrED devices resulted in a list of suggested improvements to the instructions. Implementing these improvements will make the assembly easier and result in more consistent FrED devices.

Regarding the gearbox assembly, the instructions were clear, however there was an error where one step included a video from the previous step instead of a new video. Additionally, the gearbox produced many vibrations throughout the rest of the device, which resulted in incorrect diameter readings from the camera. Adding some lubricant between the gears and minimizing tolerance variation among various printed parts will reduce the vibration, in turn resulting in more accurate measurements.

Many 3D printed parts required threaded inserts to be heat-set within the plastic. While there was a jig which pressed the inserts into the plastic, there was no standardized technique to perform this action. Many of the parts had the insert not flush with the surface of the plastic, and a key step that was missing was flattening the insert against the surface after it was pushed into the part. To solve this, it is recommended that the FrED Factory create a standard operating procedure (SOP) which can be referenced by those adding inserts into parts.

Additionally, at each subsystem station there were occasionally missing tools which were required. This was fixed by borrowing tools from other stations, but for a full factory production run it is vital that each station has all the required equipment.

Regarding the assembly of each subsystem onto the frame, and as mentioned in the methodology section, there was a lack of specificity pertaining to mounting locations of some parts. The entire camera assembly was not given a mounting location, and therefore a common pitfall in the assembly is to put it too high or low because the frame has a large quantity of available mounting positions. This was the same with the bearing locations on the camera subassembly. Specifying these locations in the instructions will improve the uniformity of each FrED.

The electronic assembly took a large amount of time because there were no instructions surrounding this. It is important that instructions for the electronics are created because the electronics are the most expensive parts of the device and they are the easiest to break if wired incorrectly. Additionally, an SOP about how to solder would be beneficial to limit errors and reduce variation between those assembling the device.

G. FrED Characterization

The characterization of FrED showcased the relevance of a stable temperature controller, which eliminates blobs in the fibre. After utilizing the PWM PI controller and the data scrubbing method to eliminate vibration noise, the normal probability plot for diameter measurements showed stochastic behavior, allowing for a full factorial DoE and ANOVA analysis. This is shown in Figure 14.

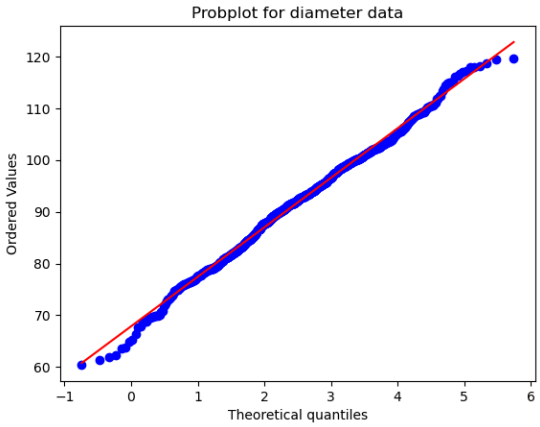

Figure 14. Normal probability plot with PWM PI temperature controller.

Furthermore, it showed that the heating current needs to be regulated to mitigate the cyclic temperature overshooting. For the current project, this was achieved with the introduction of an adjustable DC-DC buck converter, which uses the LM2596 step-down regulator from Texas Instruments. However, a better implementation would be the direct addition of the LM2596 module into the PCB, optimizing for space use and cost.

The requirement for a PWM signal to control the temperature was also concluded, allowing for higher resolution in the temperature level accuracy.

H. Full Factorial Design of Experiments

Described in the methodology, a full factorial DoE was performed to determine the effects that temperature, extruder speed, and material color have on the diameter of the fibre. The result was the linear regression model presented in Equation (12).

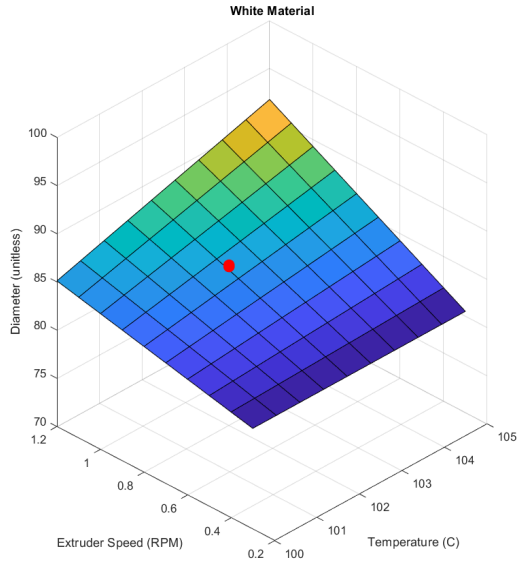

Figure 15. DoE surface response for white material.

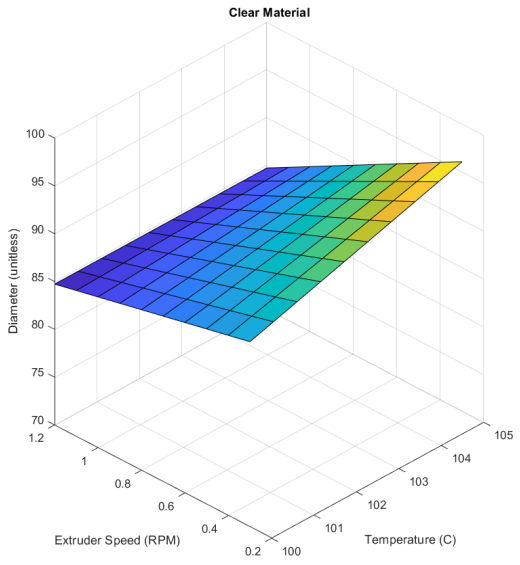

Figure 16. DoE surface response for clear material.

The surface response for the white and clear material are shown in Figures 15 and 16, respectively. Figure 15 also shows the tested quadratic point. Material color is not a scalable variable like temperature or extruder speed, and therefore it is separated into two plots so that the results can be more easily visualized.

Importantly, Equation (12) shows that temperature is only statistically significant when interacting with material color or material color and extruder speed. This is surprising, because it was hypothesized that temperature would have the largest impact on the diameter.

This discrepancy, however, can be explained due to the small range of temperatures that were tested. Because each material had a different melting temperature, only a small range of temperatures worked well with both materials. Testing each material separately with larger ranges of temperatures may provide more expected results.

The temperature variable is only significant in this model when interacting with the extruder speed variable, and this is expected because of the physical relationship that each has on the final temperature of the material. The extrusion temperature of the material is based on the temperature of the heater, as well as the time spent heating. This aligns with the hypothesis that the temperature of the material is very important when extruding to a specific diameter.

IV. Continuous Statistical Process Control

The real-time SPC addition to the FrED interface presented the possibility of monitoring the diameter's behavior. By automatically applying the 8 Nelson Rules, non-stochastic values can be identified immediately and an investigation into their causes can be performed.

An example of the SPC plot for diameter data is shown in Figure 17, where the out-of-control values (i.e. the ones that are very unlikely described by a normal distribution) are shown with red crosses, and the UCL and LCL are shown with black dotted lines.

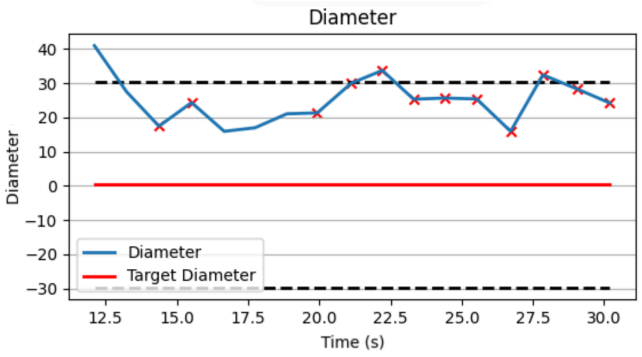

Figure 17. Example live SPC interface for diameter.

However, as discussed earlier, a final implementation requires trial runs for prolonged periods of time, establishing a diameter distribution with known mean and variance. This has to be performed on every individual FrED, unless an ANOVA analysis on different devices concludes that there are no deterministic changes between them. This result, nevertheless, would be surprising, as 3D printed parts, among other components utilized, have enough variability to make a device inoperable after the initial assembly.

As a recommendation for the acquisition of phase I data, at least two days with two or more hot melt glue tubes on each

day are advised. This would account for material-to-material changes, as well as changes that may happen between days.

Furthermore, an automated data scrubbing method needs to be implemented for data acquisition. Ideally, this method would be able to analyze image data to detect and eliminate diameter measurements corresponding to vibrations. An image preprocessing and classification pipeline could be introduced.

Preprocessing may include the application of convolutional filters that perform gradient operations - which will have low values in blurry or shaky images, as the edges blend in with the background - such as Sobel, Robert's, or Laplacian filters. Then, the entire images and/or some extracted features results can be analyzed with a classifier, such as a Support Vector Machine (SVM) and/or a Convolutional Neural Network (CNN). This method would perform as shown in Figure 18, eliminating blurry images and diameters and maintaining stable ones.

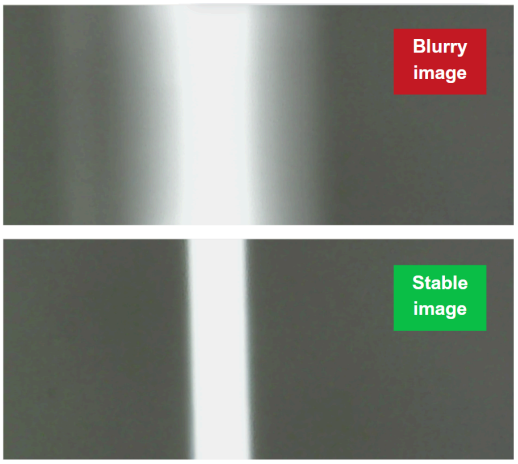

Figure 18. Example classification of blurry and stable images.

A similar classification framework is presented in [2], achieving an accuracy of 93.80% and an F1-Score 93.73%. Furthermore, the model's threshold can be tuned to minimize the false stable rate. Since false blurry results are simply accurate diameter measurements that are not utilized, they are not problematic, as the camera acquires around 10 diameter measurements per second.

With these implementations, live SPC will serve the intended purpose of detecting real non-normal behavior in the actual fibre diameter.

V. Conclusion

This project resulted in multiple improvements to the FrED device which will open the door for future projects. Ambiguity was identified within the assembly instructions, the temperature controller was redesigned, the effects of input variables were tested on the diameter output, and live statistical process control was implemented into the user interface.

Identifying areas for improvement within the FrED assembly instructions will shorten the manufacturing time of each FrED device while decreasing the variability between each device. Future work surrounding this will involve writing all missing instructions and standard operating procedures.

Redesigning the FrED temperature system to control a PWM signal with a PI controller makes the temperature much more consistent. When changing parameters the controller needs to be retuned, and therefore a future task will be identifying the optimal operating parameters and fine tuning the controller.

To ensure that the FrED was operating as expected, data was scrubbed by hand. This is one limitation of this work, as it may have unknown consequences on the results and not all behaviors may have been captured. Data scrubbing software was developed to find all instances in time where no diameter is recorded and remove a certain number of points before and after that instance to account for vibrations within the system. This did not work perfectly and therefore it is suggested that the camera subsystem be separated from the rest of the device and better vibration detection software be developed, as mentioned in the results. Implementing this may solve the issues of vibrations and focusing.

The designed experiments resulted in the surprising result that the temperature variable was not statistically significant, and therefore it is suggested that future experiments be done with the temperature variable. Specifically, testing a wider range of temperatures on only one material may provide more insightful results. Using the calculated regression model as well as future regression models, optimal parameters can be selected to make the FrED device robust and consistent.

The live statistical process control implemented into the user interface will serve to identify the user whenever the FrED device is operating unexpectedly. However, future work needs to be done to determine consistent results once the optimal parameters are selected. Using historical data to determine accurate control limits is a necessary step to make the process control work as intended.

Overall, the work done in this project will benefit the FrED Factory and serve as a base for improvement and future work.

References

[1] D. C. Montgomery, *Introduction to Statistical Quality Control*. Hoboken, N.J: Wiley, 2009.

[2] "A Simple Approach for Blur Image Detection," Medium, https://medium.com/data-science-ecom-express/a-simple-approach-for-blur-image-detection-535b3c55b5 (accessed Dec. 16, 2024).

[3] "Index," *Journal of Quality Technology*, vol. 16, no. 4, pp. 241–244, Oct. 1984. doi:10.1080/00224065.1984.11978924

[4] Ti, https://www.ti.com/lit/an/sloa293a/sloa293a.pdf?ts=1734142471135 (accessed Dec. 16, 2024).

[5] Stepper Motor Nema 17, https://pages.pbclinear.com/rs/909-BFY-775/images/Data-Sheet-Stepper-Motor-Support.pdf (accessed Dec. 16, 2024).

[6] "Home," MIT FrED Factory, https://fredfactory.mit.edu/ (accessed Dec. 16, 2024).